2014

Environmentally Persistent Free Radicals (EPFRs). 3. Free versus Bound Hydroxyl Radicals in EPFR Aqueous Solutions

Lavrent Khachatryan
Department of Chemistry, Louisiana State University, Baton Rouge

Cheri A. McFerrin
Department of Natural Sciences and Mathematics, Dominican University of California

Randall W. Hall
Department of Natural Sciences and Mathematics, Dominican University of California,
randall.hall@dominican.edu

Barry Dellinger
Department of Chemistry, Louisiana State University, Baton Rouge

Survey: Let us know how this paper benefits you.

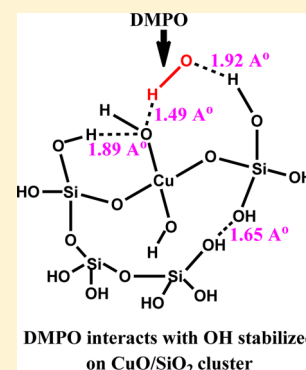# Environmentally Persistent Free Radicals (EPFRs). 3. Free versus Bound Hydroxyl Radicals in EPFR Aqueous Solutions

Lavrent Khachatryan,*,[†] Cheri A. McFerrin,[‡] Randall W. Hall,[†,‡] and Barry Dellinger[†]

[†]Department of Chemistry, Louisiana State University, Baton Rouge, Louisiana 70803, United States
[‡]Department of Natural Sciences and Mathematics, Dominican University of California, San Rafael, California 94901, United States

S Supporting Information

ABSTRACT: Additional experimental evidence is presented for *in vitro* generation of hydroxyl radicals because of redox cycling of environmentally persistent free radicals (EPFRs) produced after adsorption of 2-monochlorophenol at 230 °C (2-MCP-230) on copper oxide supported by silica, 5% Cu(II)O/silica (3.9% Cu). A chemical spin trapping agent, 5,5-dimethyl-1-pyrroline-*N*-oxide (DMPO), in conjunction with electron paramagnetic resonance (EPR) spectroscopy was employed. Experiments in spiked O^{17} water have shown that ~15% of hydroxyl radicals formed as a result of redox cycling. This amount of hydroxyl radicals arises from an exogenous Fenton reaction and may stay either partially trapped on the surface of particulate matter (physisorbed or chemisorbed) or transferred into solution as free OH. Computational work confirms the highly stable nature of the DMPO—OH adduct, as an intermediate produced by interaction of DMPO with physisorbed/chemisorbed OH (at the interface of solid catalyst/solution). All reaction pathways have been supported by *ab initio* calculations.

DMPO interacts with OH stabilized on CuO/SiO$_2$ cluster

INTRODUCTION

Resonance-stabilized, environmentally persistent free radicals (EPFRs) (semiquinone, phenoxyl, cyclopentadienyl, etc.) can form on the surfaces of fine particles and persist almost indefinitely in the environment.[1−3] Redox cycling of adsorbed EPFRs may be a source of reactive oxygen species (ROS), such as hydroxyl radicals ($^•$OH), superoxide anion radicals ($O_2^{•−}$), hydrogen peroxide (H_2O_2), etc.[1] These results were partially supported by later works.[2,4] Recently, a chemical spin trapping agent 5,5-dimethyl-1-pyrroline-*N*-oxide (DMPO) in conjunction with electron paramagnetic resonance (EPR) spectroscopy was employed to measure the production of ROS in an aqueous suspension of particle-associated EPFRs derived from adsorption of 2-monochlorophenol (2-MCP) on 5% Cu(II)O/silica (3.9% Cu) particles.[5,6] It was established that hydroxyl radicals are generated by a surface-mediated redox cycle, with the resulting hydroxyl radicals remaining completely or largely on the surface such that they cannot be readily scavenged to form secondary organic radicals in quantities detectable using currently available methods.[6] The surface-bound hydroxyl radical as well the reduced metal in the immediate vicinity are responsible for the enhanced activity of the particles. The concentration of hydroxyl radicals was measured at ~1 μM for a 140 min incubation of EPFR-containing solution.[5]

Failure to form secondary radicals using standard scavengers, such as ethanol, dimethyl sulfoxide, sodium formate, and sodium azide, suggests that caution must be used to interpret free hydroxyl radical generation in solution. There is the dilemma: first, hydroxyl radicals may form on the surface via a non-homogeneous reaction of H_2O_2 because of "site-specific OH production" known as "site-specific Fenton reaction".[7] A fraction may react with the target (in our case, with DMPO),

and the remainder may be released into solution as free OH without any significant effect on the scavengers (because of the low concentration of hydroxyl radicals). On the other hand, the significance of the concerted reaction between a metal site, H_2O_2, and a target (here DMPO) without participation of OH in the general process[7,8] cannot be excluded.

In other words, it is always challenging and in most cases unclear to ascertain the origin of OH radicals.[7,9] The large problem is that the DMPO—OH adduct (as an indicator for free OH) may also be formed by nucleophilic addition of water to DMPO catalyzed by a transition-metal impurity[10−12] (or through intermediate DMPO radical cation[13]). The non-radical nucleophilic reaction of water has been proposed to be a significant pathway for the formation of DMPO—OH radical adducts, even during a Fenton reaction;[14,15] i.e., 80–90% of the total DMPO—OH in [17]O-enriched water was due to iron-dependent nucleophilic addition of water.[15] However, the same authors also discuss a water-independent mechanism of DMPO—OH formation[15] and how an Fe or Cu ion-induced nucleophilic addition of water to DMPO may be significantly suppressed in experiments performed in most common buffers.[14]

These arguments are the main reasons for performing the spin-trapping experiments using [17]O-labeled water in the presence of EPFRs associated with CuO/SiO$_2$ nanoparticles. We provide here additional evidence of *in vitro* generation of hydroxyl radicals by EPFRs produced from the adsorption of 2-

monochlorophenol at 230 °C (2-MCP-230) on a copper oxide catalyst supported by silica nanoparticles, 5% Cu(II)O/silica (3.9% Cu).[16,17]

We use *ab initio* calculations to determine the thermodynamically favored physisorbtion/chemisorption of hydroxyl radicals on a particulate matter (PM) surface as well as illustrate the highly stable nature of the DMPO−OH adduct adsorbed at the interface of a solid catalyst in solution.

EXPERIMENTAL SECTION

Materials. High-purity DMPO (99%+, GLC) was obtained from ENZO Life Sciences International and used without further purification. 2-MCP (99+%), copper nitrate hemipentahydrate (99.9+%), and 0.01 M phosphate-buffered saline (PBS, 0.138 M NaCl/0.0027 M KCl) was all obtained from Sigma-Aldrich. Cab-O-Sil were obtained from Cabot (EH-5, 99+%). [17]O-Labeled water (40.7% [17]O, 1.6% [18]O, and 57.7% [16]O) was obtained from ICON Isotope (Summit, NJ).

EPFR Surrogate Synthesis. The 5% CuO/silica (3.9% Cu) particles were prepared by impregnation of silica powder (Cab-O-Sil) with 0.1 M solution of copper nitrate hemipentahydrate and calcined at 450 °C for 12 h.[18] The sample was then ground and sieved (mesh size of 230, 63 μm). Prior to exposure, the particles were heated *in situ* in air to 450 °C for 1 h to pretreat the surface. They were then exposed to saturated vapors of 2-MCP at 230 °C using a custom-made vacuum exposure chamber for 5 min. Once exposure was complete, the temperature of the system was cooled to 150 °C for 1 h at 10^{-2} Torr. EPR spectra were then acquired at ambient conditions to confirm the existence of EPFRs.

***In Vitro* Studies.** Both control and sample solution suspensions, containing particles without and with EPFRs, respectively, were prepared in a similar manner.[6,5] The final composition of the suspension in most experiments was particles (50 μg/mL) + DMPO (150 mM) + reagent (200 μL).

For experiments with ([17]O) H$_2$O, all reagents were dissolved in ([17]O) H$_2$O at the same concentration mentioned above [only half of the amounts of components were used to save the ([17]O)-labeled water, i.e., balanced at 100 μL].

The solutions prepared in either 100% (^{16}O) H$_2$O or 40.7% ([17]O) H$_2$O + 57.7% (^{16}O) H$_2$O were kept in the dark and shaken for 30 s using a Vortex Genie 2 (Scientific Industries) in touch mode. A total of 20 μL (10 μL in the case of [17]O-labeled water) of the solution was transferred to an EPR capillary tube (inner diameter of ∼1 mm and outer diameter of 1.55 mm) and sealed at one end with a sealant (Fisherbrand). The capillary was next inserted in a 4 mm EPR tube and placed into the EPR resonator.[19] The intensities of the EPR spectra of DMPO−OH adducts were reported in arbitrary units, DI/N [double integrated (DI) intensity of the EPR spectrum normalized (N) to account for the conversion time, receiver gain, number of data points, and sweep width].[20] Each experiment was performed at least twice, and the final intensity of the EPR spectrum of DMPO−OH represents an average of all spectra obtained for each experiment.

Because the chemistry of interaction of chelators with the surface of the model particles is unclear,[21−24] we abstained from the use of chelators, such as desferrioxamine (DFO) and diethylenetriaminepentaacetic acid (DETAPAC), which minimize the iron content in solution. The comparative method (this work), a comparison of sample and control solutions exactly at the same conditions, is preferable.[5,6] All secondary processes (DMPO decay, oxidation by dissolved oxygen,

reduction, dimerization, nucleophilic addition of water, etc.), if they occur, we believe have the same contribution for both the control and sample solutions.

EPR Measurements. EPR spectra were recorded using a Bruker EMX-20/2.7 EPR spectrometer (X-band) with dual cavities and modulation and microwave frequencies of 100 kHz and 9.516 GHz, respectively. Typical parameters were sweep width of 100 G, EPR microwave power of 10 mW, modulation amplitude of 0.8 G, time constant of 40.96 ms, and sweep time of 167.77 s.

Simulation Procedure. Bruker Win-EPR SimFonia spectral simulation program was used that runs on a personal computer (PC) under Microsoft Windows.
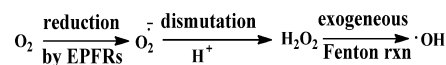
The simulation of DMPO−[16]OH gives EPR spectrum with 1:2:2:1 intensity distribution, while incorporation of [17]O atom in DMPO−OH (DMPO−[17]OH adduct) increases the number of EPR lines from 4 (for DMPO−[16]OH) to 15 (for DMPO−[17]OH) because of the [17]O coupling ([17]O has a nuclear spin of $^5/_2$),[25,26] *vide infra*. In the case of simulation for the mixture with different contents of DMPO−[17]OH/DMPO−[16]OH, the total number of lines will reach 19 (cf. panels a and b of Figure 2), with the relative intensity of each spin adduct spectra directly proportional to their percentage content.

Computational Details. *Ab initio* calculations were performed with the Gaussian 09 suite of programs.[27] The B3LYP hybrid functional was chosen because it has recently been shown consistent with experimental spin-trapping results involving DMPO[28] and provides reliable ground-state structural parameters for copper-containing structures.[29] Homolytic bond dissociation energies (BDEs) studied with a variety of density functional theory (DFT) methods also indicate B3LYP usage with a correlation-consistent basis set minimizing the deviation from benchmark calculations.[30] As a result, we used the correlation-consistent, double-ζ polarized cc-pVDZ basis set in our calculations. Each stationary-point structure (B3LYP/cc-pVDZ) yielded only real frequencies. Scaling factors for the frequencies were not applied.

RESULTS AND DISCUSSION

The hypothesized Scheme 1 may be a source of ROS generation.[5,6] It involves (1) electron transfer from the EPFR

Scheme 1

$$O_2 \xrightarrow[\text{by EPFRs}]{\text{reduction}} O_2^{\cdot -} \xrightarrow[H^+]{\text{dismutation}} H_2O_2 \xrightarrow[\text{Fenton rxn}]{\text{exogenous}} {}^{\cdot}OH$$

to molecular oxygen, forming superoxide radical ion, and (2) hydrogen peroxide and a hydroxyl radical are produced via dismutation and Fenton reactions, respectively. The spin-trapping experiments in [17]O-spiked water may spread a light on the problem of whether DMPO−OH adducts are generated by nucleophilic addition of water to DMPO or via Scheme 1.

Spin Trapping by DMPO in [17]O-Enriched Water. The results of spin-trapping experiments performed in [16]O water and [17]O-enriched water are represented in Figure 1. The intensity of DMPO−[16]OH adducts is consistently higher in sample solutions: curve 1 in comparison to the control in regular H$_2$[16]O water (not shown).[5,6] The same trend is observed for DMPO−[16]OH adducts in [17]O-enriched water: curve 2 represents the sample, and curve 2′ represents the control solutions. On the other hand, the isotopic effect on the
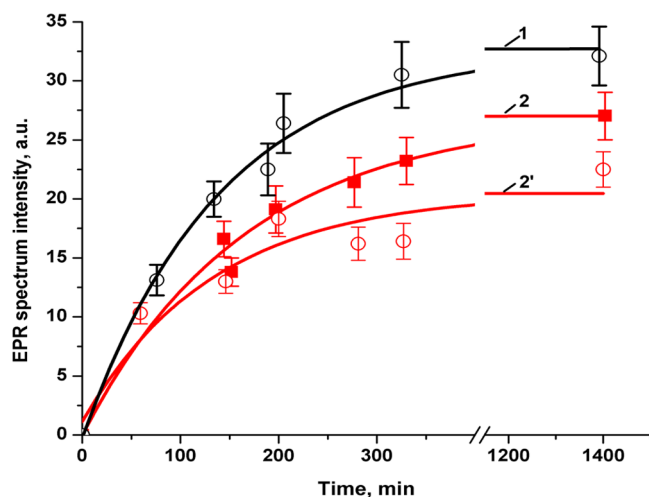
Figure 1. Difference in the DMPO−OH adduct spectral intensity for the samples containing EPFRs in ^{16}O water (line 1) and ^{17}O-enriched water (line 2). Line 2′ stands for control solution in ^{17}O-enriched water.

accumulation of spin adducts is clearly seen; i.e., the DMPO−^{16}OH spectra intensity in water with composition of 40.7% (^{17}O) H_2O + 57.7% (^{16}O) H_2O is less than in 100% ^{16}O water (lines 2 and 1 in Figure 1, respectively). The difference between sample, curve 2, and control solutions, curve 2′ (currently ~15−20% at high incubation time), can be markedly increased after centrifuging the sample by removing large clusters in the particle solution. The smaller the size of the nanocluster, the higher the activity to generate ROS.[31] As a result, a 40−50% difference can be seen between sample and control solutions, unambiguously showing the fact of generation of hydroxyl radicals during redox cycling.

Finally, while the characteristic four lines of the DMPO−OH spectrum were typical for the EPFR solution prepared in 100% ^{16}O water,[6] a modified EPR spectrum was detected in EPFR solution prepared in water with composition of 40.7% (^{17}O)

H_2O + 57.7% (^{16}O) H_2O (black and red lines in Figure 2a). The extra nuclear hyperfine splitting observed in Figure 2a is due to the DMPO−^{17}OH adduct[14] [15 lines with hyperfine splitting constant (hsc) = 4.66 G for ^{17}O, which has a nuclear spin, $I = \frac{5}{2}$] along with DMPO−^{16}OH (4 lines with hsc = 15.0 G for H and N, where ^{16}O has no nuclear spin, $I = 0$). The appearance of DMPO−^{17}OH splitting is only indicative for nucleophilic addition of water on the DMPO.[15,32] These extra lines are clearly seen in simulated spectra in Figure 2b at composition of 80% (^{17}O) H_2O + 20% (^{16}O) H_2O mixture with superposition of DMPO−^{16}OH (assigned by asterisks) and DMPO−^{17}OH (rest of the 15 lines) adducts.

When simulated spectrum C (in Figure 2a) at composition of 40.7% (^{17}O) H_2O + 57.7% (^{16}O) H_2O is subtracted from the experimental spectrum B, a residue spectrum B−C is shown, which is typical for the DMPO−^{16}OH adduct EPR spectrum. The residue B−C spectrum shows that there is an additional source of formation of DMPO−^{16}OH, which is not due to the nucleophilic addition of water to DMPO and may be likely due to Scheme 1. A simple examination for the amount of residue spectrum in overall spectral intensity of experimental spectrum B (Figure 2a) demonstrated that ~85% of the oxygen atoms present in the DMPO−OH adduct originated through nucleophilic addition of H_2O to DMPO, while ~15% DMPO−^{16}OH adduct was due to the trapping of the hydroxyl radical formed from the superoxide ($^{16}O_2^{\bullet -}$) dismutation reaction (Scheme 1).

The idea that most contribution in spin-trapping experiments is produced by the addition of water to DMPO, as mentioned above, is not without literature precedence.[25,33] Ultimately, the pathway of the water-independent mechanism for DMPO−OH adduct formation must always be checked.[15]

The next question of interest is whether hydroxyl radicals produced from the exogenous Fenton reaction (site-specific Fenton reaction[7]) stay on the surface or leave it? This problem (free versus bound OH radical) was partly addressed in our previous publication.[6] It is also a dispute theme in the literature.[7,34−41]
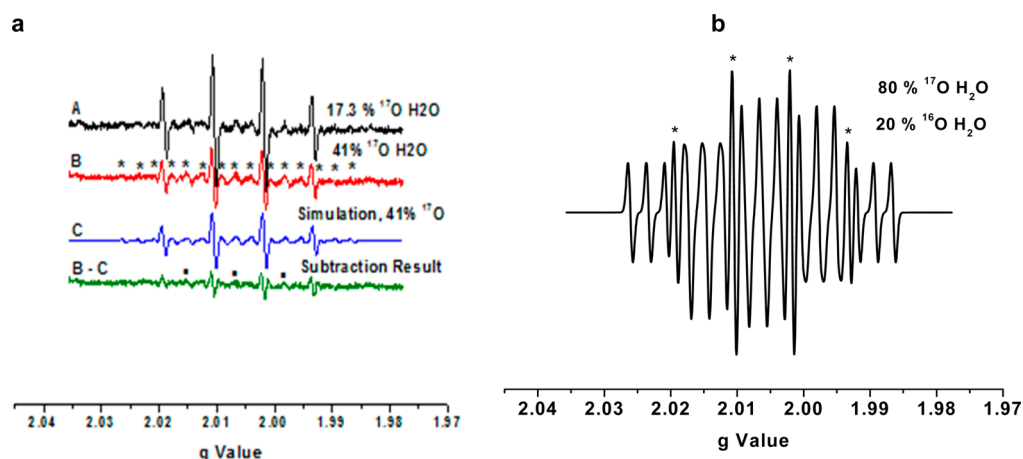

Figure 2. (a) EPR spectra of DMPO−^{17}OH/DMPO−^{16}OH adducts at an incubation time of 300 min for a solution of EPFRs (50 μg/mL) + DMPO (150 mM) + PBS (total 100 μL) with content of 17.3% (^{17}O) H_2O (black line A) and ~41% (^{17}O) H_2O (red line B). Line C is a computer simulation of DMPO−^{17}OH/DMPO−^{16}OH adducts at a concentration of 41% ^{17}O and 59% ^{16}O based on the parameters from panel b. B−C is the residue spectrum where the 3 lines assigned by squares represent the EPR spectrum for ^{15}N (~0.37% isotopic abundance in nature). (b) Computer simulation of the DMPO−^{17}OH/DMPO−^{16}OH adduct EPR spectrum at a concentration of 80% ^{17}O and 20% ^{16}O in water (the spectrum assigned by an asterisk corresponds to DMPO−^{16}OH). The hsc values for N and H are ~15.01 and 4.66 G for ^{17}O. g, 2.0061; ΔH_{p-p}, 1.15 G; and the EPR line shape, Gaussian.
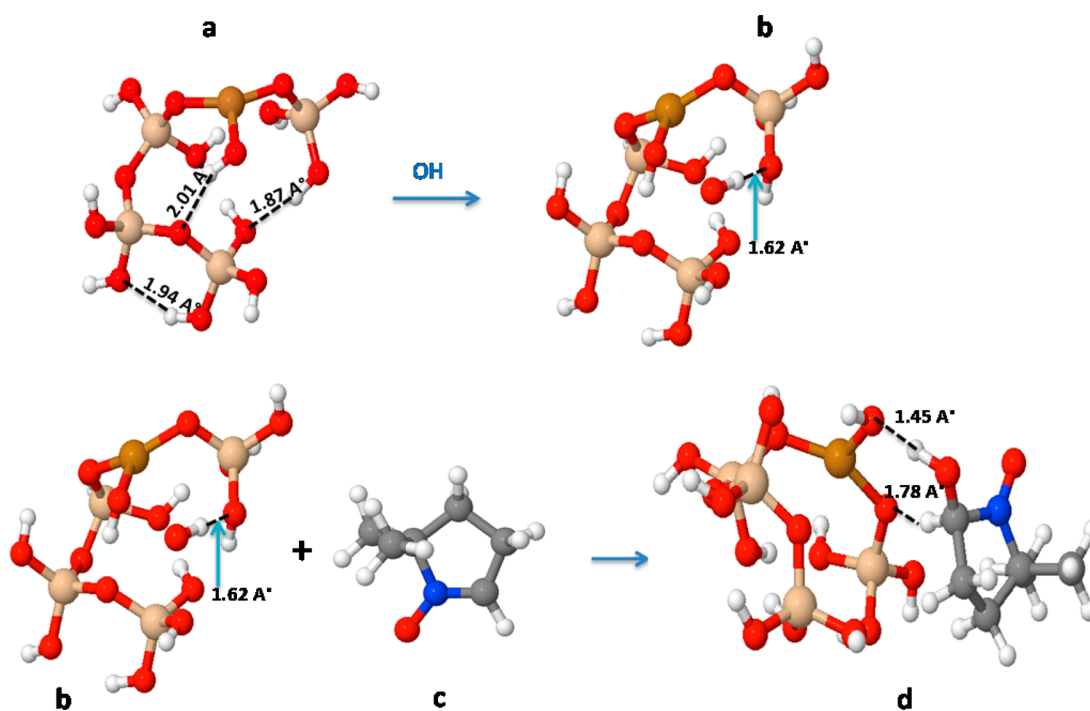
Figure 3. Illustration of the (a) chained-shaped cluster with trigonal planar form of Cu, (b) adsorption (trapping) of OH because of hydrogen bonding shown by the arrow on the CuO/SiO$_2$ surface, and (c and d) further interaction of the cluster with DMPO (C, brown; N, blue; O, red; and H, white). Dark gray, Cu; light gray, Si; red, O; white, H.
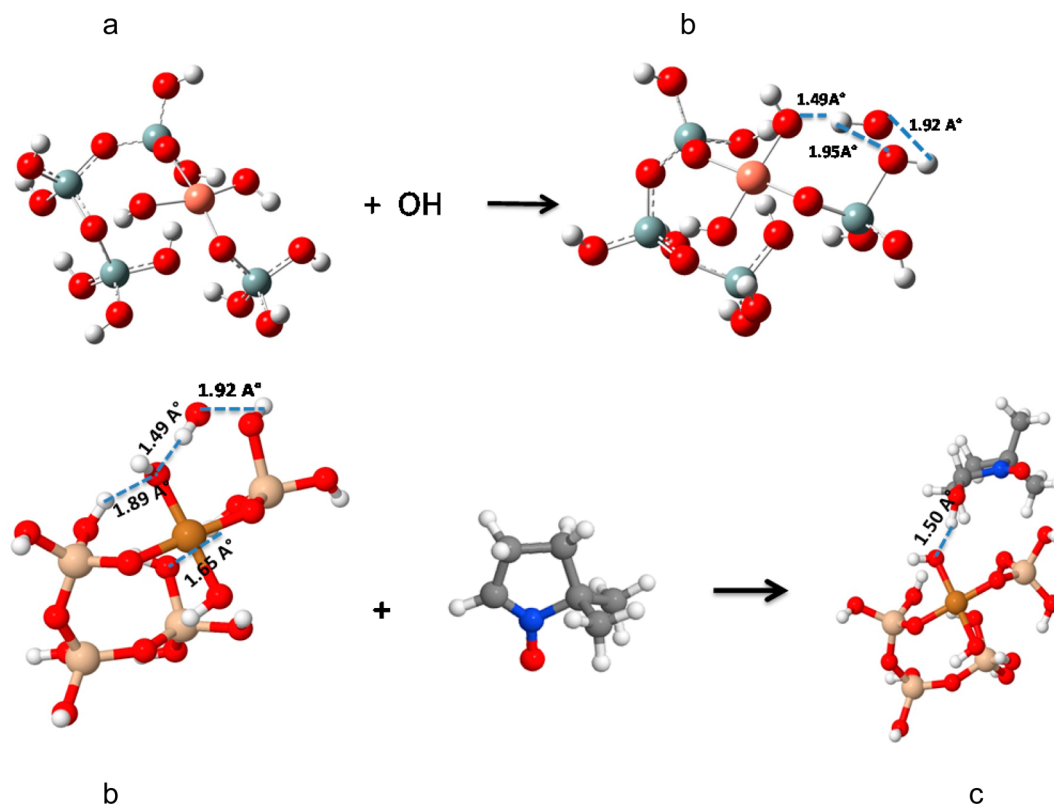

Figure 4. (a) Adsorption of OH on cluster (tetrahedral Cu) and (b) interaction of DMPO (black, C; blue, N; red, O; white, H) with adsorbed OH by (c) formation of stabilized DMPO−OH on cluster surfaces. The hydrogen bonding is shown by dashed lines. Dark gray, Cu; light gray, Si; red, O; white, H.

One of the plausible experimental facts of surface site bound OH is deduced from the high stability of the DMPO−OH adduct (days) at the interface of solid catalyst/solution.[6] This

experimental fact is surprising. For comparison note, the half-life time of DMPO−OH in homogeneous media depends upon the environment and may be changed from 2 to 20 min

(aqueous solution)[12,42] or 55 min in phosphate buffer.[43] A long lifetime is only reported in ref 44: the DMPO−OH spin adducts in water solution last for hours depending upon the temperature.

In fact, it may be emphasized that the portion of DMPO−OH-formed in an independent way (from the addition of OH to DMPO) is stable likely on the silica surfaces or the catalyst site. There is literature experimental data about stabilization of DMPO adducts on secondary organic aerosol particles such as DMPO−HO₂, DMPO−RO, DMPO−RO₂, and DMPO−OH detected by electrospray ionization−tandem mass spectrometry (ESI−MS/MS)[45] and DMPO−glutathionyl in an intracellular environment using high-performance liquid chromatography (HPLC).[46]

To address the existence of surface site bound OH as well as high stability of DMPO−OH in an environment of CuO/SiO₂, *ab initio* calculations were initiated. The calculations were used to assess the thermodynamic basis for the current interpretation of experimental results by hypothesizing the following: (1) Because of EPFRs cycling mechanism the H₂O₂ is formed at the interface of nanoparticle/water solution.[5,6] The hydroxyl radicals may be generated by either an exogenous Fenton reaction[5,6,47] or by direct decomposition of H₂O₂ on the surface sites, defects (see the Supporting Information). (2) The hydroxyl radicals are stabilized by surface-active centers. (3) DMPO attacks stabilized (physisorbed/chemisorbed) OH radicals, forming a DMPO−OH adduct, which stays on the surface for a long time because of energetic stabilization.

CuO/SiO₂ Model Systems with Both Trigonal- and Tetrahedral-Coordinated Cu Sites. We have performed *ab initio* calculations to investigate the stabilization (physisorption and chemisorption) of OH radicals on model CuO/SiO₂ surfaces, followed by further interaction of the adsorbed OH with DMPO. Note that physisorption of the OH radical is primarily characterized by the hydrogen bonding taking place (the bonding distance of ≤2 Å), whereas chemisorption is characterized by the absence of hydrogen bonding (the bonding distance close to the covalent bond value of, for instance, in HO−OH, ~1.45−1.47 Å).

Experimental synthesis of copper-containing silicates reveals a mixture of copper in each of its valence states.[48,48,49] X-ray photoelectron spectroscopy (XPS) reveals the presence of copper hydroxide, copper oxide, and Si−O−Cu bonds in these clusters. While Chang et al. argue that the stable Si−O−Cu bonds are primarily electrostatic,[48] Parameswaran et al. suggest that their stable nature is covalent.[49]

Our model reactant surface is a copper-containing silica-like structure derived from the addition of a −O−Cu−(OH)₂ moiety to the previously optimized tetrahedrally-coordinated, radical hydroxide cluster found by Kubicki et al.[41] [Figures 3a (3-coordinate Cu) and 4a (*vide infra* tetrahedral Cu cluster)].

Radical-ended, as opposed to ionic, silica-like structures have been computationally shown to add water favorably via a radical silicate−water mechanism, as opposed to a cationic or anionic silicate mechanism, with both radical pathways (H₂O + •SiO or SiO•) resulting in a hydroxylated silica surface site.[41] We have considered a limited number of atoms around an active site to make the calculations tractable, as small models have been used successfully by other researchers.[50,51,41]

The optimized Cu atoms in structures a and b of Figure 3 are both incorporated into a trigonal planar geometry, with Cu−OH and Cu−O bond distances similar to experimental values.[52,53] Small inorganic Cu(I) and Cu(II) complexes have

been experimentally found to exhibit both trigonal and tetragonal coordination around the Cu atom.[54−58] As a result, we also added a hydroxyl moiety to the 3-coordinate Cu cluster (directly to Cu atom) shown in Figure 3a to produce a 4-coordinate Cu cluster (in Figure 4a). The addition of OH to the 3-coordinate Cu clusters yields reaction energy of −33.2 kcal/mol.

The hydrogen bonds arranged in both head-to-tail and intramolecular fashion shown in both Figures 3b and 4b allow for the physisorption of OH (Figure 3b; bond distance of 1.62 Å) with an exoergic reaction energy of $\Delta E = -21.95$ kcal/mol or chemisorption of reactive hydroxyl groups (Figure 4b; bond distance of 1.49 Å) with an exoergic reaction energy of −29.5 kcal/mol.

Further addition of DMPO to the physisorbed/chemisorbed hydroxyl radicals in Figures 3b and 4b is also exoergic, leading to the stabilization and formation of the DMPO−OH adduct, for instance in Figure 3d, with an exoergic reaction energy of −86.7 kcal/mol. The addition of DMPO to the chemisorbed OH in Figure 4b also yields an exoergic reaction energy of −73.2 kcal/mol. Stabilization of DMPO−OH because of hydrogen bonding on the cluster surface is shown in Figures 3d and 4c. It has been shown recently that DMPO and inorganic radicals favor radical addition over nucleophilic addition in the presence of hydrogen bonding, both experimentally and computationally.[28]

These theoretical calculations complement experimental evidence for the highly stable nature of DMPO−OH adducts in CuO/SiO₂ aqueous solutions.

Therefore, the integrated intensity of DMPO−OH adducts may be considered a sum of DMPO−OH formed from the addition of free OH (because of the exogenous Fenton reaction generated by the cycle) to DMPO and a portion of DMPO−OH stabilized on a particle surface (as a result of the attack of DMPO to OH trapped on the surface). Currently, the DMPO−OH adducts formed in a solution or on the surfaces of particles are not distinguishable. We may hypothesize that the rate of accumulation of DMPO−OH adducts on particle surfaces decreases during incubation because of sluggish generation of OH; i.e., the initial EPFRs as well as reductants are consumed in secondary reactions not generating additional amounts of OH in the cycle. Because DMPO−OH decays faster in solution, we conclude that the surface-stabilized DMPO−OH adducts are responsible for the longer incubation times. In addition, the surface-stabilized DMPO−OH adducts are not expected to return to solution because the exoergicity of the reactions for both a trigonal planar Cu (Figure 3) and a tetrahedral Cu (Figure 4) are sufficiently high at −86.7 and −73.2 kcal/mol, respectively.

Our calculations also show that DMPO may interact with physisorbed or chemisorbed hydroxyl groups on the CuO/SiO₂ cyclic cluster surfaces with the release of DMPO−OH into solution (see the Supporting Information). As a consequence, there may be multiple hydroxyl-radical-generating pathways: (i) The mayor channel of OH generation is the cycling scheme of EPFR proposed earlier.[5,47] OH forms through the exogenous Fenton reaction as follows:

$$H_2O_2 + Cu(I)\ (\text{organic ligand})$$
$$\rightarrow Cu(II)\ (\text{organic ligand}) + OH^- + OH^\bullet \qquad (1)$$
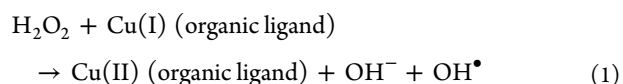
Hydroxyl radicals formed in reaction 1 are either partially transferred into solution and form homogeneously DMPO−

OH adducts or partially stabilized on the particle surfaces, forming DMPO−OH stable adducts (Figures 3 and 4). (ii) *Ab initio* calculations show that a partial decomposition of H_2O_2 on the silica surface active sites is also possible. For instance, because of homolytic cleavage of H_2O_2 on the silica active sites (defects, dangling bonds, etc.), one hydroxyl group hydroxylates the surface site (chemisorption) and the second hydroxyl radical is trapped between neighboring Si−OH groups on the surface (by hydrogen bonds) (see Figure S1B of the Supporting Information). Further experimental addition of DMPO leads to stabilization and formation of DMPO−OH on the surfaces (Figure S2 of the Supporting Information).

■ ASSOCIATED CONTENT

Ⓢ Supporting Information

Data about the addition of OH and H_2O_2 to the tetrahedral form of Cu in CuO/SiO₂ model systems (cyclic structure) and computational details about direct decomposition of H_2O_2 on silica active sites. This material is available free of charge via the Internet at http://pubs.acs.org.

■ AUTHOR INFORMATION

Corresponding Author
*Telephone: 225-578-4417. E-mail: lkhach1@lsu.edu.
Notes
The authors declare no competing financial interest.

■ ACKNOWLEDGMENTS

■ REFERENCES

(1) Squadrito, G. L.; Cueto, R.; Dellinger, B.; Pryor, W. A. Quinoid redox cycling as a mechanism for sustained free radical generation by inhaled airborne particulate matter. *Free Radical Biol. Med.* **2001**, *31* (9), 1132−1138.

(2) Valavanidis, A.; Fiotakis, K.; Bakeas, E.; Vlahogianni, T. Electron paramagnetic resonance study of the generation of reactive oxygen species catalyzed by transition metals and quinoid redox cycling by inhalable ambient particulate matter. *Redox Rep.* **2005**, *10* (1), 37−51.

(3) Dellinger, B.; Lomnicki, S.; Khachatryan, L.; Maskos, Z.; Hall, R.; Adounkpe, J.; McFerrin, C.; Truong, H. Formation and stabilization of persistent free radicals. *Proc. Combust. Inst.* **2007**, *31*, 521−528.

(4) Alaghmand, M.; Blough, N. V. Source-dependent variation in hydroxyl radical production by airborne particulate matter. *Environ. Sci. Technol.* **2007**, *41* (7), 2364−2370.

(5) Khachatryan, L.; Vejerano, E.; Lomnicki, S.; Dellinger, B. Environmentally persistent free radicals (EPFRs). 1. Generation of reactive oxygen species (ROS) in aqueous solutions. *Environ. Sci. Technol.* **2011**, *45*, 8559−8566.

(6) Khachatryan, L.; Dellinger, B. Environmentally persistent free radicals (EPFRs). 2. Are free hydroxyl radicals generated in aqueous solutions? *Environ. Sci. Technol.* **2011**, *45*, 9232−9239.

(7) Sutton, H. C.; Winterbourn, C. C. On the participation of higher oxidation states of iron and copper in Fenton reactions. *Free Radical Biol. Med.* **1989**, *6* (1), 53−60.

(8) Zhang, G. Y.; Long, J. L.; Wang, X. X.; Zhang, Z. Z.; Dai, W. X.; Liu, P.; Li, Z. H.; Wu, L.; Fu, X. Z. Catalytic role of Cu sites of Cu/MCM-41 in phenol hydroxylation. *Langmuir* **2010**, *26* (2), 1362−1371.

(9) Bataineh, H.; Pestovsky, O.; Bakac, A. pH-Induced mechanistic changeover from hydroxyl radicals to iron(IV) in the Fenton reaction. *Chem. Sci.* **2012**, *3* (5), 1594−1599.

(10) Burkitt, M. J.; Tsang, S. Y.; Tam, S. C.; Bremner, I. Generation of 5,5-dimethyl-1-pyrroline *N*-oxide hydroxyl and scavenger radical adducts from copper/H_2O_2 mixtures—Effects of metal ion chelation and the search for high-valent metal−oxygen intermediates. *Arch. Biochem. Biophys.* **1995**, *323* (1), 63−70.

(11) Finkelstein, E.; Rosen, G. M.; Rauckman, E. J. Spin trapping of superoxide and hydroxyl radical—Practical aspects. *Arch. Biochem. Biophys.* **1980**, *200* (1), 1−16.

(12) Makino, K.; Hagiwara, T.; Murakami, A. Fundamental aspects of spin trapping with DMPO. *Radiat. Phys. Chem.* **1991**, *37* (5−6), 657−665.

(13) Singh, R. J.; Karoui, H.; Gunther, M. R.; Beckman, J. S.; Mason, R. P.; Kalyanaraman, B. Reexamination of the mechanism of hydroxyl radical adducts formed from the reaction between familial amyotrophic lateral sclerosis-associated Cu,Zn superoxide dismutase mutants and H_2O_2. *Proc. Natl. Acad. Sci. U. S. A.* **1998**, *95* (12), 6675−6680.

(14) Hanna, P. M.; Chamulitrat, W.; Mason, R. P. When are metal ion-dependent hydroxyl and alkoxyl radical adducts of 5,5-dimethyl-1-pyrroline *N*-oxide artifacts. *Arch. Biochem. Biophys.* **1992**, *296* (2), 640−644.

(15) Chamulitrat, W.; Iwahashi, H.; Kelman, D. J.; Mason, R. P. Evidence against the 1−2−2−1 Quartet DMPO spectrum as the radical adduct of the lipid alkoxyl radical. *Arch. Biochem. Biophys.* **1992**, *296* (2), 645−649.

(16) Truong, H. Copper(II) oxide mediated formation and stabilization of combustion generated persistent free radicals. Ph.D. Dissertation, Department of Chemistry, Louisiana State University, Baton Rouge, LA, 2007.

(17) Lomnicki, S.; Truong, H.; Vejerano, E.; Dellinger, B. Copper oxide-based model of persistent free radical formation on combustion-derived particulate matter. *Environ. Sci. Technol.* **2008**, *42* (13), 4982−4988.

(18) Truong, H.; Lomnicki, S.; Dellinger, B. Potential for misidentification of environmentally persistent free radicals as molecular pollutants in particulate matter. *Environ. Sci. Technol.* **2010**, *44* (6), 1933−1939.

(19) Nakagawa, K. Is quartz flat cell useful for the detection of superoxide radicals? *J. Act. Oxygens Free Radicals* **1994**, *5*, 81−85.

(20) Eaton, G. R.; Eaton, S. S.; Barr, D. P.; Weber, R. T. *Quantitative EPR*; Springer-Verlag: Berlin, Germany, 2010; pp 185.

(21) Fubini, B.; Mollo, L.; Giamello, E. Free radical generation at the solid/liquid interface in iron containing minerals. *Free Radical Res.* **1995**, *23* (6), 593−614.

(22) Tomita, M.; Okuyama, T.; Watanabe, S.; Watanabe, H. Quantitation of the hydroxyl radical adducts of salicylic acid by micellar electrokinetic capillary chromatography—Oxidizing species formed by a Fenton reaction. *Arch. Toxicol.* **1994**, *68* (7), 428−433.

(23) Yamazaki, I.; Piette, L. H. EPR spin-trapping study on the oxidizing species formed in the reaction of the ferrous ion with hydrogen peroxide. *J. Am. Chem. Soc.* **1991**, *113* (20), 7588−7593.

(24) Zhu, B. Z.; Har-El, R.; Kitrossky, N.; Chevion, M. New modes of action of desferrioxamine: Scavenging of semiquinone radical and stimulation of hydrolysis of tetrachlorohydroquinone. *Free Radical Biol. Med.* **1998**, *24* (5), 880−880.

(25) Zhang, H.; Joseph, J.; Felix, C.; Kalyanaraman, B. Bicarbonate enhances the hydroxylation, nitration, and peroxidation reactions catalyzed by copper, zinc superoxide dismutase—Intermediacy of carbonate anion radical. *J. Biol. Chem.* **2000**, *275* (19), 14038−14045.

(26) Lloyd, R. V.; Hanna, P. M.; Mason, R. P. The origin of the hydroxyl radical oxygen in the Fenton reaction. *Free Radical Biol. Med.* **1997**, *22* (5), 885−888.

(27) *Gaussian*, 2009; http://www.gaussian.com/g_tech/g_ur/m_citation.htm.

(28) Zamora, P. L.; Villamena, F. A. Theoretical and experimental studies of the spin trapping of inorganic radicals by 5,5-dimethyl-1-pyrroline *N*-oxide (DMPO). 3. Sulfur dioxide, sulfite, and sulfate radical anions. *J. Phys. Chem. A* **2012**, *116* (26), 7210−7218.

(29) De Luna, P.; Bushnell, E. A. C.; Gauld, J. W. A density functional theory investigation into the binding of the antioxidants ergothioneine and ovothiol to copper. *J. Phys. Chem. A* **2013**, *117* (19), 4057−4065.

(30) Rijs, N. J.; Brookes, N. J.; O'Hair, R. A. J.; Yates, B. F. Theoretical approaches to estimating homolytic bond dissociation energies of organocopper and organosilver compounds. *J. Phys. Chem. A* **2012**, *116* (35), 8910−8917.

(31) Kiruri, L. W.; Khachatryan, L.; Dellinger, B.; Lomnicki, S. Effect of copper oxide concentration on the formation and persistency of environmentally persistent free radicals (EPFRs) in particulates. *Environ. Sci. Technol.* **2014**, *48*, 2212−2217.

(32) Makino, K.; Hagiwara, T.; Hagi, A.; Nishi, M.; Murakami, A. Cautionary note for DMPO spin trapping in the presence of iron ion. *Biochem. Biophys. Res. Commun.* **1990**, *172* (3), 1073−1080.

(33) Alegria, A. E.; Ferrer, A.; Sepulveda, E. Photochemistry of water-soluble quinones. Production of a water-derived spin adduct. *Photochem. Photobiol.* **1997**, *66* (4), 436−442.

(34) Tojo, S.; Tachikawa, T.; Fujitsuka, M.; Majima, T. Oxidation processes of aromatic sulfides by hydroxyl radicals in colloidal solution of TiO_2 during pulse radiolysis. *Chem. Phys. Lett.* **2004**, *384* (4−6), 312−316.

(35) Hodgson, E. K.; Fridovich, I. Interaction of bovine erythrocyte superoxide dismutase with hydrogen peroxide—Inactivation of enzyme. *Biochemistry* **1975**, *14* (24), 5294−5299.

(36) Hodgson, E. K.; Fridovich, I. Interaction of bovine erythrocyte superoxide dismutase with hydrogen peroxide—Chemiluminescence and peroxidation. *Biochemistry* **1975**, *14* (24), 5299−5303.

(37) Lawless, D.; Serpone, N.; Meisel, D. Role of OH radicals and trapped holes in photocatalysis. A pulse radiolysis study. *J. Phys. Chem.* **1991**, *95* (13), 5166−5170.

(38) Donaldson, K.; Brown, D. M.; Mitchell, C.; Dineva, M.; Beswick, P. H.; Gilmour, P.; MacNee, W. Free radical activity of PM_{10}: Iron-mediated generation of hydroxyl radicals. *Environ. Health Perspect.* **1997**, *105*, 1285−1289.

(39) Venkatachari, P.; Hopke, P. K.; Brune, W. H.; Ren, X. R.; Lesher, R.; Mao, J. Q.; Mitchel, M. Characterization of wintertime reactive oxygen species concentrations in Flushing, New York. *Aerosol Sci. Technol.* **2007**, *41* (2), 97−111.

(40) Chen, X.; Hopke, P. K.; Carter, W. P. L. Secondary organic aerosol from ozonolysis of biogenic volatile organic compounds: Chamber studies of particle and reactive oxygen species formation. *Environ. Sci. Technol.* **2011**, *45* (1), 276−282.

(41) Narayanasamy, J.; Kubicki, J. D. Mechanism of hydroxyl radical generation from a silica surface: Molecular orbital calculations. *J. Phys. Chem. B* **2005**, *109* (46), 21796−21807.

(42) Khan, N.; Wilmot, C. M.; Rosen, G. M.; Demidenko, E.; Sun, J.; Joseph, J.; O'Hara, J.; Kalyanaraman, B.; Swartz, H. M. Spin traps: In vitro toxicity and stability of radical adducts. *Free Radical Biol. Med.* **2003**, *34* (11), 1473−1481.

(43) Barriga, G.; Olea-Azar, C.; Norambuena, E.; Castro, A.; Porcal, W.; Gerpe, A.; Gonzalez, M.; Cerecetto, H. New heteroaryl nitrones with spin trap properties: Identification of a 4-furoxanyl derivative with excellent properties to be used in biological systems. *Bioorg. Med. Chem.* **2010**, *18* (2), 795−802.

(44) Buettner, G. R.; Oberley, L. W. Considerations in spin trapping of superoxide and hydroxyl radical in aqueous systems using 5,5-dimethyl-1-pyrroline-1-oxide. *Biochem. Biophys. Res. Commun.* **1978**, *83* (1), 69−74.

(45) Pavlovic, J.; Hopke, P. K. Detection of radical species formed by the ozonolysis of *α*-pinene. *J. Atmos. Chem.* **2010**, *66* (3), 137−155.

(46) Stoyanovsky, D. A.; Goldman, R.; Jonnalagadda, S. S.; Day, B. W.; Claycamp, H. G.; Kagan, V. E. Detection and characterization of the electron paramagnetic resonance-silent glutathionyl-5,5-dimethyl-1-pyrroline *N*-oxide adduct derived from redox cycling of phenoxyl radicals in model systems and HL-60 cells. *Arch. Biochem. Biophys.* **1996**, *330* (1), 3−11.

(47) Dellinger, B.; Khachatryan, L.; Masko, S.; Lomnicki, S. Free radicals in tobacco smoke. *Mini-Rev. Org. Chem.* **2011**, *8* (4), 427−433.

(48) Huang, C.-C.; Wu, M.-S.; Chen, C.-L.; Li, Y.-B.; Ho, K.-C.; Chang, J.-S. Preparation of silica particles doped with uniformly dispersed copper oxide nano-clusters. *J. Non-Cryst. Solids* **2013**, *381*, 1−11.

(49) Sivasubramanian, G.; Shanmugam, C.; Parthasarathi, B.; Parameswaran, V. R. XPS characterization and bactericidal properties of a biomass derived silica−copper nanocomposite. *Adv. Sci., Eng. Med.* **2013**, *5*, 342−348.

(50) Sauer, J.; Ugliengo, P.; Garrone, E.; Saunders, V. R. Theoretical study of van der Waals complexes at surface sites in comparison with the experiment. *Chem. Rev.* **1994**, *94* (7), 2095−2160.

(51) Murashov, V. Ab initio cluster calculations of silica surface sites. *J. Mol. Struct.* **2003**, *650* (1−3), 141−157.

(52) Persson, I.; Pennerhahn, J. E.; Hodgson, K. O. An EXAFS spectroscopic study of solvates of copper(I) and copper(II) in acetonitrile, dimethyl sulfoxide, pyridine, and tetrahydrothiophene solutions and a large-angle X-ray scattering study of the copper(II) acetonitrile solvate in solution. *Inorg. Chem.* **1993**, *32* (11), 2497−2501.

(53) Frank, P.; Benfatto, M.; Szilagyi, R. K.; D'Angelo, P.; Della Longa, S.; Hodgson, K. O. The solution structure of $[Cu(aq)]^{2+}$ and its implications for rack-induced bonding in blue copper protein active. *Inorg. Chem.* **2005**, *44* (6), 1922−1933.

(54) Bernhardt, P. V.; Bramley, R.; Engelhardt, L. M.; Harrowfield, J. M.; Hockless, D. C. R.; Korybutdaszkiewicz, B. R.; Krausz, E. R.; Morgan, T.; Sargeson, A. M.; Skelton, B. W.; White, A. H. Copper(II) complexes of substituted macrobicyclic hexaamines—Combined trigonal and tetragonal distortions. *Inorg. Chem.* **1995**, *34* (14), 3589−3599.

(55) Burdett, J. K.; Eisenstein, O. From 3-coordination to 4-coordination in copper(I) and silver(I). *Inorg. Chem.* **1992**, *31* (10), 1758−1762.

(56) Texter, J.; Strome, D. H.; Herman, R. G.; Klier, K. Chemical and spectroscopic properties of copper containing zeolites. *J. Phys. Chem.* **1977**, *81* (4), 333−338.

(57) Teraoka, Y.; Tai, C.; Ogawa, H.; Furukawa, H.; Kagawa, S. Characterization and NO decomposition activity of Cu-MFI zeolite in relation to redox behavior. *Appl. Catal., A* **2000**, *200* (1−2), 167−176.

(58) Olsson, M. H. M.; Ryde, U.; Roos, B. O.; Pierloot, K. On the relative stability of tetragonal and trigonal Cu(II) complexes with relevance to the blue copper proteins. *J. Biol. Inorg. Chem.* **1998**, *3* (2), 109−125.